Foamed lignin-silicone bio-composites by extrusion then compression molding

Journal:	*Green Chemistry*
Manuscript ID:	GC-ART-06-2015-001418.R1
Article Type:	Paper
Date Submitted by the Author:	28-Jul-2015
Complete List of Authors:	Zhang, Jianfeng; McMaster University, Chemistry and Chemical Biology Fleury, Etienne; INSA Lyon,, Ingénierie des Matériaux Polymères Brook, Michael A.; McMaster University, Chemistry and Chemical BIology

Green Chemistry

ARTICLE

Foamed lignin-silicone bio-composites by extrusion then compression molding

Received 00th January 20xx,
Accepted 00th January 20xx

DOI: 10.1039/x0xx00000x

www.rsc.org/

Jianfeng Zhang,[a] Etienne Fleury[b] and Michael A. Brook[a*]

The use of lignin, one of the most abundant natural products, has not gained wide use as a feedstock due to the difficulty of processing it. We have developed a simple route to produce lignin-silicone composite foams via first extrusion and then compression molding. The formulation consists of raw lignin particles, suitable mixtures of hydrosilanes, and the catalyst $B(C_6F_5)_3$. In order to balance the reaction rates between extrusion and molding, as well as find other optimized conditions for producing foamed structures, a series of optimizations established that a uniform, closed cell lignin-silicone foam was most effectively made by extrusion at room temperature followed by molding at elevated temperatures under pressure for up to 5 minutes. The morphology and uniformity of the foamed structure depended on many factors, including the quantity of lignin, catalyst, the crosslinking silicone PHMS, the molecular weight of the spacer silicone H-PDMS-H, and the molding temperature. The content of lignin, acting as both reinforcing filler and crosslinker (chemically bonded to the siloxane network), could be varied over a wide range from 25 to 55%. The mechanical performance of the lignin-silicone foams was characterized using DMA and tensile tests (tensile strength up to 0.42 MPa, break-at-elongation up to 249%). The strength of the foam was improved by post-curing at 140 °C. Although the lignin-silicone foam loses some elasticity after post-curing, it maintains reasonable stability even after heating to 300 °C for 12 h. This processing method for lignin-based bio-composites provides new opportunities for better utilization of lignin in silicones and more broadly in organic materials.

Introduction

There is an increasing trend to the utilization of sustainable and renewable natural resources. Biomass,[1, 2] particularly cellulose, has been widely used in many fields, such as the food, paper, plastics, and pharmaceutical industries.[3-5] Lignin, the network polymer that glues polysaccharidic moieties together, is far less utilized due to difficulties with its processing.[6] Unlike cellulose that has well defined structure based on glucose, lignin is a highly crosslinked and branched polymer without well-defined repeating units.[7, 8] Lignin makes up about 18 ~ 35% by weight in wood; and the estimated available annual production could be over 20 million tons as the byproduct of paper industry.[9, 10] Currently, lignin is mostly used as a low value fuel (~ 150 USD/ton for industrial lignin)[11]; an important exception is the industrial production of the flavoring agent vanillin.[12, 13]

Lignin has been blended into, or copolymerized with, other polymers to create composites. It acts as a filler in polymers such as in polyurethanes,[14-19] epoxies,[20-23] and phenolics,[24, 25] among others.[10, 19, 26-30] However, most of the methods require the lignin to be pre-modified before use to improve the interfacial interaction between lignin and the polymer matrix. Such additional steps are disadvantageous in industrial processes. Lignin-based polyurethane foams, the best studied lignin-filled composites, have been explored extensively.[31-38] These foams exhibit excellent thermal and mechanical properties, with lignin content of up to 30 weight%. Although the preparation of urethanes using MDI (diphenylmethane diisocyanate) avoids a pre-modification step, the toxicity of this compound is also a drawback.

Extrusion and compression molding are common processing techniques used in the plastics industry to mix polymer formulations and then create objects: these processes have also been used for biomass processing and modification.[39-42] The techniques allow the processing to be performed at a flexible scale without the need for solvents. Various polymers, like PVA (poly(vinyl alcohol)),[43] starch,[44] and HDPE (high density polyethylene)[45] have been blended with lignin using reactive extrusion. Lignin has also been extruded

[a] Chemistry and Chemical Biology, McMaster University, 1280 Main St. W., Hamilton, Ontario, Canada L8S 4M1. Fax: +1-(905) 522-2509; Tel: +1-(905) 525-9140 ext. 23483; E-mail: mabrook@mcmaster.ca.
[b] Université de Lyon, CNRS, UMR 5223, INSA-Lyon, IMP@INSA, F-69621, Villeurbanne, France. Fax: +33-472-438-527; E-mail: etienne.fleury@insa-lyon.fr.

† Electronic Supplementary Information (ESI) available: drawing of the equipment used for measuring evolved gas during the reaction, formulations used in preliminary studies, disintegration of foam and hydrolysis of Si-H in KOH 1-butanol solutions, kinetics of hydrogen production in preliminary studies, crosslinked lignin-silicone material formed in extruder, comprehensive cross-sectional images of lignin-silicone foams made from the formulations discussed in this paper, photo of one product (not processable using extrusion and molding) made from a formulation with high viscosity, a method for preparation ATR-IR samples, ATR-IR and NMR spectra, complete information for Si-H conversion% of the lignin-silicone foams, TGA curves for lignin, elastomer, and lignin-silicone foams (F-4 and F-10) under a nitrogen atmosphere and DMA data for selected lignin silicone foams. See DOI: 10.1039/x0xx00000x

together with silicone and silica.[46] However, in these cases the lignin was used simply as a non-reinforcing filler with no effort to establish a favorable interfacial interaction between lignin and silicone matrix.

Recently, our group developed a method to efficiently decompose or modify lignin using hydrosilanes, catalyzed by $B(C_6F_5)_3$ (BCF, tris(pentafluorophenyl)borane) – the Piers-Rubinsztajn (PR) reaction.[47, 48] The process leads to the conversion of phenol, arylmethoxy groups, and other ethers into alkyl groups or silyl ethers (Scheme 1A).[49] As a consequence, the lignin surface becomes siliconized, rendering it much more compatible with hydrophobic polymers. This permitted the use of raw softwood lignin as a reinforcing/crosslinking filler in silicone elastomers in a one step process.[50] The resulting lignin-silicone elastomer has excellent mechanical properties, even when filled with as much as 40 weight% lignin.

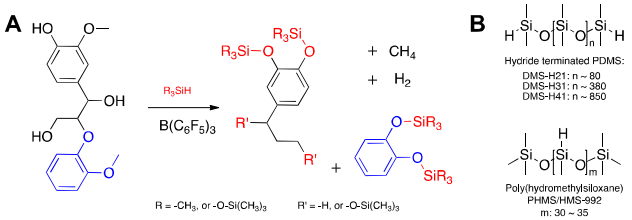

Scheme 1. (A) Typical reactions at phenolic linkages in lignin. (B) The chemical structures hydride-terminated PDMS (H-PMDS-H) and poly(hydromethylsiloxane) (PHMS).

The formation of lignin/silicone elastomers required the participation of solvent and reduced pressure in order to remove the gas produced during the reaction.[50-52] While the evolution of gas can cause vacancies/defects in an elastomer, it can be useful for generating foamed materials. We describe a simple and effective method to make foamed lignin-silicone biocomposites via extrusion and compression molding. Although silicone foams are widely used for cushioning, thermal and electrical insulation and protective applications,[53] large scale applications are still blocked by the high cost of silicones and challenges in making foams reproducibly when using alcohols/water as co-blowing agents.[54] In our research, the expensive silicone was diluted and reinforced/filled with raw lignin, which accounted for up to 55 weight% in the composite.

Experimental

Materials

Decamethylcyclopentasiloxane (D_5) and hydride-functional silicones, including hydride-terminated PDMS (H-PDMS-H, DMS-H21, H31, and H41, with molecular weights of 6000, 28000, and 62700 g/mol, respectively) and poly(hydromethylsiloxane) (PHMS, HMS-992, Mw = 1800 ~ 2100 g/mol) were purchased from Gelest (for structures see Scheme 1B). The catalyst $B(C_6F_5)_3$ (Sigma-Aldrich) was dissolved in dry toluene to provide a stock solution (40 mg/ml, 78.13 mM). Anhydrous toluene, cyclohexane, 1-butanol, and KOH (potassium hydroxide) were purchased from Sigma-Aldrich and used without purification. Softwood kraft lignin was obtained from Weyerhaeuser or Sigma Aldrich. The lignins were used as received without further drying or processing.

Lignin-silicone foam fabrication - optimization of conditions and formulations

Preliminary optimizations: a series of preliminary optimization studies were performed in solution to obtain appropriate conditions and formulations that could be used during the extrusion process. The concentration of Si-H groups (hydrosilane) before and after mixing serves as a surrogate for reactivity (a separate set of experiments measured residual Si-H in the final, cured product, see below). A gas meter was used to measure the volumes of gas released during the reaction (ESI†). The flask and U shaped gas meter were immersed in either an oil or water bath to maintain a constant temperature. The hydrosilanes (DMS-H31 mixed with PHMS) were stored in a 1 ml syringe. (*NOTE: The gaseous products can evolve very rapidly and, are comprised of flammable constituents including hydrogen, methane and other organic materials. Caution should be exercised. Avoid a closed system and use proper ventilation* with *no nearby sources of ignition.*) Other reagents, including lignin, BCF, and D_5, were premixed and heated to the target temperature in the flask; the valve was left open for at least 15 min to avoid a potential gas expansion error caused by heating. The reaction started once the hydrosilanes were injected into the flask. The valve was closed immediately to collect and measure the volume of gas produced. The gas volume was recorded against time. Four parameters including catalyst concentration, hydrosilane concentration, temperature, and the order of feeding were studied. The studies are detailed in the ESI† and show that efficient reactions could be induced at temperatures up to 90 °C with catalyst concentrations ranging from 1000-4000 ppm and lignin content of about 50 weight%.

Extrusion and compression molding of lignin-silicone foam: The lignin-silicone foam mixture was made using a micro-extruder (DMS Micro 15 cc Twin-screw Compounds) and then a compression-molding instrument (TECHMO, clamping force up to 6 tons and heating temperature up to 200 °C, respectively), as shown in Scheme 2. The optimized order of feeding lignin into the injector was determined from preliminary studies. For extrusions, half of the portion of the lignin powder (~ 3 g) was premixed with BCF solution (~ 0.5 ml) to which the H-PDMS-H (~ 7.7 g) was added. The mixture was then added to the upper feeding hopper after the extruder had reached 100 rpm. PHMS (~ 1.2 g, from the upper feeding hopper), mixed with the second half portion of lignin (~ 3 g, from the side hopper), was added after 15 s. The mixture was allowed to mix in the extruder for 3 min. A mold was placed under the outlet to collect the mixture, which was then immediately transferred to the preheated compression molding (holding at 90 °C for periods ranging from 5 min up to

3 h, under 1 ton pressure). Several conditions and formulations were tested (Table 1). For the F-4 formulations, compression molding processes were performed at 60, 90 and 120 °C.

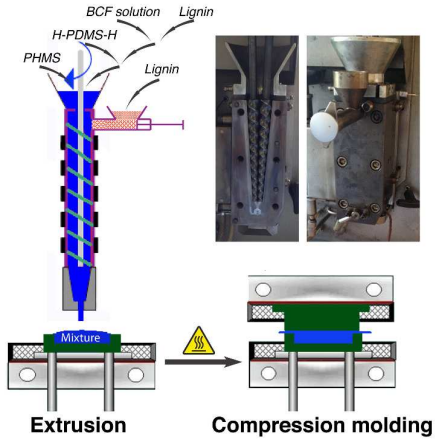

Scheme 2. Illustration of the extrusion and compression molding process. The inset images show the cross-section and assembled views of micro-scale twin-extruder.

Changes in the foam as a function of cure time in the compression mold were determined: ~300 mg samples were cut from molded foam samples after curing for 5, 15, 30, 60, and 180 min, respectively. The samples were characterized using ATR-FTIR, and then extracted in cyclohexane (~ 50 ml) for 12 h. The weight loss of the sample was calculated from the mass before and after extraction. NMR measurements were taken of the extracts from F-3, F-2 (5 min), and F-4 (5 min) (after removal of the solvent by evaporation).

Table 1. Parameters used to optimize extrusion and molding conditions, and formulations for lignin-silicone foam.

No.	Lignin		PHMS		H-PDMS-H		BCF /ppm	Molding temperature /°C	Resultant foam structure[a]
	Mass /g	wt %	Mass /g	wt %	Type	Mass /g			
F-1	6.2	41	1.2	8	H31	7.7	300	90	A2
F-2	6.2	41	1.2	8	H31	7.7	1000	90	A1
F-3	6.2	41	1.2	8	H31	7.7	1350	90	A1
F-4 A	6.2	41	1.2	8	H31	7.7	2050	60	A1
F-4 B	6.2	41	1.2	8	H31	7.7	2050	90	B2[c]
F-4 C	6.2	41	1.2	8	H31	7.7	2050	120	A1
F-5	6.2	41	0.6	4	H31	8.3	2050	90	A1
F-6	6.2	41	2.4	16	H31	6.5	2050	90	C2
F-7	6.2	41	3.6	24	H31	5.3	2050	90	C2
F-8	2.25	15	0.65	4.4	H31	12	2050	90	A1
F-9	3.75	25	0.75	5	H31	10.5	2050	90	B1[c]
F-10	8.25	55	1.6	10	H31	5.15	2050	90	C1
F-11	6.2	41	1.2	8	H25	7.7	2050	90	A1
F-12	6.2	41	1.2	8	H41	7.7	2050	90	-[d]
F-13	6.2	41	1.2	8	Mix[b]	7.7	2050	90	B1[c]

[a] The type of foam structures are illustrated in Fig. 1. [b] Mix = 26% H25, 48% H31, and 26% H41. [c] Foams with homogeneous porous structure and satisfactory mechanical performance. [d] No foam was obtained due to the extreme high intrinsic viscosity of precursor.

Hydrolysis of Si-H groups during compression molding

Loss of Si-H groups in solvent was used to show the degree of reaction that could be expected in the extruder (above). The degree of reaction in the second processing step, compression molding, was following by hydrolyzing residual Si-H groups in the cured foam (ESI†). The cured lignin-silicone foam (~ 400 mg) was sliced into thin layers (dimension: 0.5 mm × 5 mm × 10 mm) and soaked in 1-butanol (15 ml). The suspension was placed in a 50 ml round-bottomed flask and placed in an oil bath (30 °C) for 20 min, while the valve was kept open. To start the test, 2 ml of a saturated KOH solution in 1-butanol was injected from the syringe; at the same time, the valve was closed and the gas collected. The reaction was allowed to run for at least 30 min until the thin foam layer had lost its integrity (ESI†). Theoretically, 37.41 ml of gas would be produced from 1 g of PHMS by this method. Therefore, the conversion of Si-H was calculated by using followed equation:

$$Conversion_{Si-H}\ \% = \frac{Volume_{collected\ gas}}{Mass_{foam\ layer} \times wt\%_{PHMS} \times 37.42} \times 100\%$$

where the $Volume_{collected\ gas}$ is read from the experimental setup, the $Mass_{foam\ layer}$ is the weight of sliced thin layer dispersed in 1-butanol: the $wt\%_{PHMS}$ for different formulations may be found in Table 1.

Characterization

ATR-FTIR (attenuated total reflectance infrared spectroscopy, Thermo Scientific Nicolet iS10) and ^{1}H NMR spectra (Bruker Avance 400 MHz nuclear magnetic resonance spectrometer with 32 scans for 1H NMR, ESI†) were also used to characterize Si-H conversion and curing progress during composite fabrication. FTIR spectra were normalized to the characteristic peak for silicone (Si-Me @ ~1250 cm^{-1}), the (high) concentration of which is essentially fixed. ATR-FTIR spectra were run on at least three different positions on a sample.

The modulus and elongation-at-break of lignin-silicone foams were determined using a Universal Test System (INSTRON 3300, 300 N load cell). The foam sheet was cut into a dumbbell shape (according to French Standard NF T51-034, H2) and clamped with grips at both ends. The crosshead speed of stretching was set for 20 mm/min. An electronic digital micrometer (EG100, Onosokki; 0.001-mm sensitivity) was used to measure the average thickness and width of the tested specimens at three random positions. The samples were not run under humidity-controlled conditions, as the ambient humidity of the lignin itself was ~4% (from TGA measurements, data not shown).

Thermogravimetric analysis (TGA, TA instruments Q500) was run under air (flow rate = 100 ml/min) from 50 - 800 °C with a 10 °C /min step for a sample weighted around 20 mg. Dynamic mechanical analysis (DMA, Triton, Germany) was performed under compression mode with the frequency of 1 Hz, sinusoidal displacement of 0.2 mm and heating rate of 1 °C/min. The tested samples were punched as a disk (dimensions: diameter = 10 mm, and thickness = 3 mm). The

glass transition temperature (Tg) was determined from the peak temperature of the damping (tan δ) curve. The morphologies of foam cross-sections were imaged using a digital single-lens reflex camera with macro view mode (Canon T3).

Results and discussion

Optimal foam structures

Visually, foams are materials containing dispersed voids. They are characterized by overall bubble density, and the homogeneity of bubble size and shape. Preliminary experiments revealed the approximate conditions and formulations necessary to generate foams using mixtures of BCF, lignin, and silicone hydrides (see ESI† for details). Two steps were used in the process: formulations were first extruded at room temperature to give a homogenous mixture; in the second stage, the extruded lignin-silicone precursor was compression molded at elevated temperatures to give foamed composite. A few classes of foams produced during model studies are representative of the rest of the foams discussed below. To facilitate that discussion, three typical foams types are presented in Fig. 1: the "foam" exhibiting large and randomly sized voids (Type A), closed cell foams with uniform morphology (Type B), and solid foams with trapped bubbles and fewer defects (Type C). Foams of Type A1 are generally easy to break, and have domains either very soft or hard. Type C foams are more rigid than the other two types. However, type B foams are of particular interest because of their excellent insulating properties.[55] Following a summary of the chemistry used to blow the foams, the ability to control foam structure by varying both processing conditions and formulations will be presented.

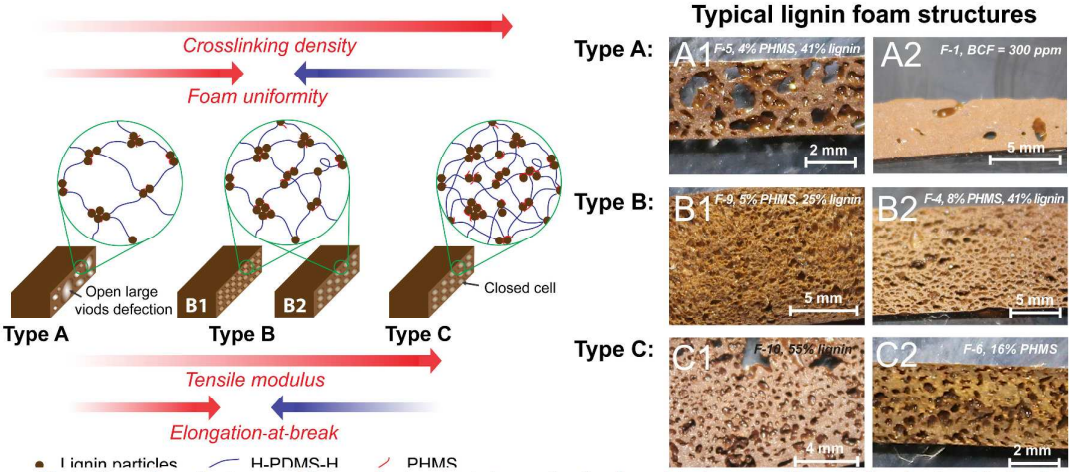

Fig. 1 Illustrations of lignin-silicone foam structures, and their resultant mechanical properties: tensile modulus increases with crosslinking density, while the elongation-at-break are depended on both crosslinking density and uniformity of foams. Type A structures are foams either with large trapped (A1) or collapsed voids (A2, closer to an elastomer than a foam); Type A1 foams are easy to break with extension or bending due to the large defects. Type B structures are foams with uniform morphology; these foams are flexible with tunable toughness. Types C are foams with excessive crosslinking density and fewer voids; Type C1 foams are tough, while Type C2 were brittle.

Chemistry at the lignin-silicone interface

The reaction between hydrosilanes and lignin in the presence of $B(C_6F_5)_3$ can lead to elastomers and, in the absence of diluents, foams. Two reactions are involved in the process: the reaction between lignin and hydrosilane to 'siliconize' the lignin surface, and crosslinking of the silicone. Both of these reactions produce gas, primarily hydrogen from OH groups, and methane from ArOMe groups, with other alkanes formed in low concentration (Scheme 1, and Scheme 3). The spontaneously generated gases can act as perfect in-situ blowing agents for foam fabrication if molding conditions can be properly managed.

Lignin has rich quantity of -OH and ether linkages available for reaction (see ESI† FT-IR of lignin);[15, 17, 19] we found from our previous study that, depending on dispersion of lignin particles in the matrix, about 0.8 - 11 μmol/mg reactive functional groups located at interface.[50] Optimizing the process for any given lignin, therefore, requires determining the density of these functional groups on the lignin particle surface: both hard and softwood lignin can lead to foams.

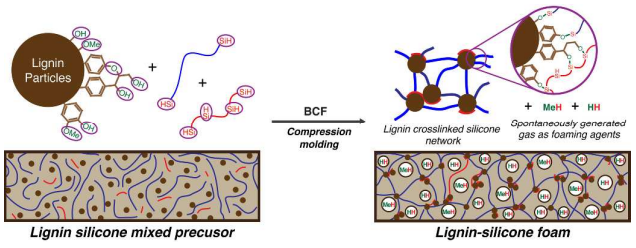

Scheme 3. The chemistry at lignin interface: silylation and crosslinking during the compression molding processing.

Optimization of formulations and processing conditions for lignin-silicone foam

One objective of this research was to establish if, while controlling foam structure, the materials could be compression molded into desired shapes after mixing the ingredients in an extruder: mixing rather than chemistry should occur in the extruder. Fortunately, during the extrusion process, the reaction rate for condensation between aryl ether/hydroxyl and hydrosilane is expected to be relatively slow until uniform mixing of the components is achieved, particularly if the materials are not heated. By contrast, during (heated) compression molding the reaction rate is expected to be fast.

During the chemical grafting process (designed to take place during compression molding), the reduction of phenol, alcohol, and methoxy groups at the lignin surface by hydrosilanes results in large volume of gas being produced (Scheme 3). Because the gas is trapped in the volume-confined mold, a foamed lignin-silicone composite is produced. The nature of the foamed structure is determined by the competition between crosslinking (and attendant viscosity build) and gas production. Several key factors were examined, including formulation: catalyst loading; crosslinker (lignin) and co-crosslinker (PHMS) concentrations; and molecular weight of the H-PDMS-H). Reaction conditions including temperature and feeding order of reagents, were also investigated during extrusion and compression molding to better understand the relationship between the process and foam structure.

Optimization of the formulation. *Catalyst loading:* The impact of catalyst loading on reaction rate is straightforward: higher reaction rates of gas generation and crosslinking were observed with increasing loading. The preliminary studies examined catalyst loading from 300 ppm to 2000 ppm. At higher loadings, e.g., 4000 ppm, the reaction is too fast to control, with induction time less than 30 seconds. In addition, excess catalyst led to scabbing in the channel of extruder (ESI†).

Distinct foam structures were formed as a function of catalyst loading. At lower catalyst loading (300 ppm), the composite presented as a solid elastomer rather than a foam (Type A2 in Fig. 1). More uniform foams formed at higher catalyst loadings (BCF = 1000, and 1350 ppm, ESI†). A uniform foam with small, regular and dispersed voids was produced with 2050 ppm BCF (Type B2 in Fig. 1). In our view, the properties of such closed cell, homogeneous closed cell homogeneous foams are most desirable and optimization methods were developed to lead to such materials

These results are readily understood as a consequence of the competition between curing and gas production. Both rates were low at lower catalyst loadings. Therefore, the gas can escape at a rate comparable with its production during molding process, leaving the upper portion of the mold unfilled and a low porosity product (ESI†). Porous structures required higher catalyst loadings, when both the curing and gas production rates increased.

Lignin (crosslinker) and PHMS (co-crosslinker) content: Lignin, as shown in Scheme 3, acts as both polyfunctional crosslinker and filler in the formulation. PHMS, while also acting as flexible crosslinker, is primarily responsible for the formation of hydrogen and alkane by-products and the concomitant crosslinking that occurs during foaming (Scheme 3). As a consequence, the lignin and PHMS concentrations controlled the rates of crosslinking.

Lignin, the extrusion/molding optimizations demonstrated that foams with a uniform structure could be made with lignin contents ranged from 25 to 55% (Types B1, B2, and C1 in Fig. 1), although some defects were found with foams containing 55% lignin: mixtures with higher lignin contents also proved more difficult to extrude.[56] The viscosity of the uncured, mixed precursor increases with direct correlation to lignin content, simply due to an increase in the solid fraction in the mixture. Formulations with lower lignin content (F-8, 15%) led to foams with Type A1 structure (Fig. 1, ESI†) due to the slower build in viscosity that facilitated gas escape.

PHMS, foams with non-uniform and large vacancies resulted when insufficient PHMS was present (4wt%, ESI†), mainly due to the slower rate of gas production. By contrast, foams with uniform pores were obtained within an appropriate range of PHMS content (from 8 to 24wt%). The porous structure of these foams was uniform, but subtle changes in PHMS concentrations led to differences in specific morphologies (e.g., both Types B2 and C2 in Fig. 1, were made within this PHMS concentration range, ESI†). Foams with the more desirable closed and uniform structure (Type B) were made from formulations with intermediate PHMS content (~8%).

Molecular weight of H-PDMS-H: As noted above, viscosity could be used as an effective tool for tailoring foam morphologies by varying lignin content. H-PDMS-H served as a spacer that reduced crosslink density and an additional way to manipulate viscosity. This ingredient was varied with respect to the chain length of the PDMS spacer. Foams with uniform porous structures (Type B1 and B2 in Fig. 1) were only obtained when intermediate viscosities were used, either by choosing a spacer of appropriate chain length (F-4B, $Mw_{silicone\ spacer}$ = 28,000 g/mol), or by mixing different H-PDMS-H spacers with a distribution of chain lengths (F-13, $Mw_{silicone\ spacer}$ 6,000 to 62,700 g/mol, Table 1, ESI†). By contrast, low viscosities that accompanied the use of 6,000 g/mol H-PDMS-H resulted in a Type A1 structure (F-11, Fig. 1, Table 1, ESI†), and use of high molecular weight spacers (F-12, Mw 62,700 g/mol) led to mixtures that were too viscous to mix and extrude (ESI†). Therefore, the optimal formulations for Type B foams were F-4B, F-9, and F-13 (Table 1).

Optimizations with respect to processing. The foam generation process involves two steps: mixing in an extruder, and curing in a compression mold (under different temperatures and holding times). The conditions for each of these steps needed to be optimized in light of the chemical steps taking place. There is normally an induction time for the Piers-Rubinsztajn reaction and the feeding order of reagents

impacts the length of that induction time. Substances such as water, alcohol, or other impurities found in lignin can form adducts with $B(C_6F_5)_3$, retarding the rate of the desired reaction:[57, 58] there may be other factors that affect reaction induction. Thus, the timing of the extrusion and holding time/compression steps must be coordinated with these chemical factors.

Mixing order: In preliminary studies, the induction time varied with feed order (ESI†). When BCF was premixed with lignin prior to the addition of the hydrosilanes (Mixing order A), longer induction times and slower initial reaction rates resulted. By contrast, shorter induction times and rapid reaction rates were observed if hydrosilanes were premixed with lignin in prior to adding BCF (Mixing order B). As a slow reaction rate is desired in the first step, "Mixing order A" was adopted as the standard feeding order for preliminary studies, and also for the extrusions.

Temperature: Similar to the impact of catalyst loading, increasing temperature resulted in decreased induction times, while increased reaction rates. In preliminary optimizations using a solution system, not an extruder, a high conversion% of PHMS (more than 50%, as shown by gas evolution) was reached within 300 s at 90 °C (ESI†); by contrast, less than 10% of PHMS was reacted after 1500 s at 30 °C. Therefore, for the extrusion step, lower temperature is desired.

During compression molding, the mixture from extruder developed strength and shape (against the mold surface) while curing, which was also affected by temperature. The properties and performance of resultant materials depended on the curing progress. In our test, incomplete cure was shown by the presence of extractable polymers that had not grafted into the foam network, and which could be removed by cyclohexane extraction. Although cured foams were *obtained* over the whole tested temperature range from 60 to 120 °C (after holding for 5 minutes, see below for other holding times), the quantities of extractable substances were not linear with temperature (Table 2). Either higher (120 °C) or lower (60 °C) molding temperatures resulted in higher ratios of extractable substances. This outcome at low temperatures is readily understood: the reaction rate was so slow that unbound hydrosilane remained. By contrast, the fast reaction rate at higher molding temperatures caused immediate gelation, capturing domains of uncured cured materials.

Foam morphology was also affected by molding temperature. Desirable uniform foam structures were observed at intermediate temperatures (90 °C, F-4B, BCF = 2050 ppm, Type B2 in Fig. 1), whereas non-uniform sized and randomly distributed bubbles (Type A1 in Fig. 1, ESI†) were produced at either lower (60 °C) or higher (120 °C) molding temperatures with identical formulations (F-4A and C, BCF = 2050 ppm). At lower molding temperatures, primary bubbles had time to coalesce at a rate comparable to cure, leading to large and randomly sized bubbles, while at higher temperatures, uncontrolled rapid foaming occurred at the start of reaction, again leading to large voids. As noted above, inhomogeneity led to significant quantities of extractables at this temperature.

Holding time: In general, samples were allowed to cure for 5 minutes during compression molding. Longer holding times were not beneficial as shown using F-3 as an example. The Si-H signal (ATR-IR) was reduced significantly after 5 minutes curing at 90 °C (ESI†), but only a very subtle decrease (~ 5% of peak area) of Si-H signal was observed after additional holding times. Similarly, solvent extraction (Table 2, ~ 2% decrease in extractables) and NMR tests (no Si-H was detected after 15 minutes) showed very small changes after this time (ESI†). Thus, there is no benefit to molding for longer times than 5 minutes. Note that a portion of the extractables may have resulted from partially depolymerized fragments from softwood lignin rather than silicones.[48]

Table 2. The weight formation (%) of lignin-silicone foams after extraction with cyclohexane

No.	Molding temperature /°C	BCF /ppm	Polymer yield (weight% residual foam after extraction) after different holding periods				
			5 min	15 min	30 min	60 min	180 min
F-1	90	300	- [a]	- [a]	- [a]	63	93
F-2	90	1000	81	89	89	90	91
F-3	90	1350	82	90	91	91	92
F-4 A	60	2050	87	88	88	89	91
F-4 B	90	2050	89	90	90	90	92
F-4 C	120	2050	83	84	84	84	86

[a] Extraction failed because the uncured lignin-silicone precursor was a liquid or paste.

Post-curing out of the mold: Si-H groups are susceptible to both oxidation and hydrolysis, leading to the formation of Si-OH groups that, in turn can condense ($R_3SiH \rightarrow R_3SiOH \rightarrow R_3SiOSiR_3$). These processes provide a secondary mechanism for crosslinking once the foam is removed from the mold. As these changes have the potential to impact the mechanical and other properties of resultant lignin-silicone foam (e.g., flammability), it was essential to quantitate the residual Si-H groups and eliminate them as much as possible via an extra post-curing process.

The concentration of residual Si-H groups in cured foams was determined by collecting the gas emitted, hydrolyzing the foam in a KOH/1-butanol solution (Table 3, ESI†). The degree of Si-H secondary cure through oxidation/hydrolysis exhibited a strong dependence on post-curing temperature (Table 3, ESI†). To test this proposal, a post-curing process was applied to sample made from F-4, a foam with good morphological qualities, at a higher temperature than that used during compression. It should be noted that post-curing had no impact on foam morphologies, since the foam structure had been set during compression molding. However, post cure increased the moduli through additional curing. As shown in Table 3, the storage modulus increased with samples that had been posted cured near 140 °C for 12 hours (see below). However, compared with post curing at 140 °C, higher post-curing temperatures (> 170 °C) led to degraded mechanical performance. There was no benefit at higher temperatures. The conversion % of Si-H was significantly increased, up to 79%, after post-curing beyond 170 °C, which is the critical

point for lignin degradation (TGA, see ESI†) and repolymerization.[59] Weight loss and homogenous shrinkage in all dimensions were observed for samples post-cured beyond 170 °C (volume shrinkage: > 8% at 220 °C, and ~ 20 % at 300 °C).

Table 3. The conversion ratio of Si-H in lignin-silicone foam after post-curing at higher temperature, and their mechanical performance

Post-curing		Weight loss %	Conversion of Si-H[a] %	E' @ T_m + 50 °C /MPa	E'' @ T_m + 50 °C /MPa
T/°C	Time/h				
Control[b]		0	43	0.54	0.13
140	12	0	44	1.2	0.16
220	5	8	69	1	0.15
	12	16	77	0.67	0.073
300	12	20	79	0.52	0.025

[a] The error of this test is about 5%. [b] no post-curing was applied at higher temperature.

Mechanical properties of lignin-silicone foams

The mechanical properties of lignin-silicone foam were measured by tensile tests and dynamical mechanical analysis (DMA, Table 4, and ESI†). Lignin – in the form of rigid particles – provides reinforcement for the otherwise soft silicone foam, altering the mechanical properties. Also, the morphologies of the foamed structures themselves were shown to strongly impact the mechanical performance of the foams.

DMA: A typical DMA curves for the lignin-silicone foams, including changes of tan δ (tan delta, red), storage (E', blue), and loss (E'', green) modulus with temperature, are shown in Fig. 2. Similar to other silicone materials: the glass transition (T_g) was found near -112 °C;[60] cold crystallization was observed in a range from -100 to -90 °C;[61, 62] the melting of silicone (T_m) occurred within the range from -42 to -36 °C.[62-64] The E' and E'' (storage and loss moduli, respectively) in unreinforced silicones decreased continuously in the glassy region.[64, 65] The storage and loss moduli of the lignin-reinforced foam stayed almost constant between -90 to -50 °C in exactly the same way as commercial silica-reinforced silicone materials.[61, 62] More importantly, a significant improvement of the storage modulus in the rubbery region was observed with lignin reinforcement ranging from 0.3 to 17 MPa (ESI†), values that are comparable to some silica-reinforced silicone materials (usually found in the range from 1 to 10 MPa).[62, 64]

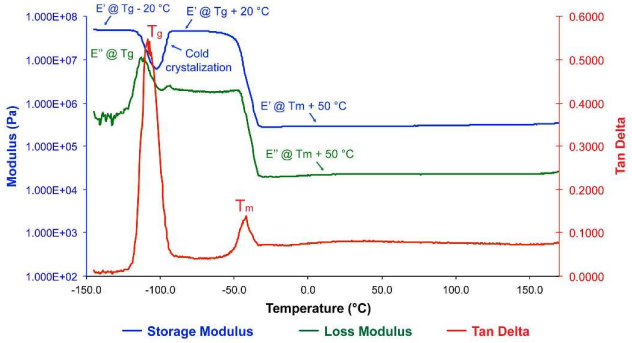

Fig. 2 The reprehensive DMA curves of lignin-silicone (F-9).

The impact of crosslinking density on mechanical performance (at a molecular level): the storage modulus increases proportionally to crosslinker density ($\rho = E'_{@T_g+50\ °C}/3RT$).[66] At the rubbery region, the storage modulus was found to increase with both lignin and PHMS content (DMA, ESI†): as lignin content increased for 25 to 55wt%, E' went from 0.29 to 3 MPa; as the other crosslinker PHMS increased from 8 to 24wt%, E' increased from 0.54 to 17 MPa. The storage modulus of samples with even lower crosslinking density (15% lignin or 4% PHMS) did not follow this rule, however, due to the large voids present.

The impact of polymer network structure on mechanical performance (at a microscopic level): The glass transition temperatures (T_g) of lignin-silicone foam were found to be comparable to the T_g (-119 °C) of an end-linked silicone network (ESI†),[62, 67] implying the network of which the foam is composed has particles bridged by chains derived from H-PDMS-H spacer silicones. The foams prepared with excess PHMS (F-6 and 7) were found to have higher T_g (ESI†), due to the increasing fraction of a secondary crosslinker in the network, and these materials were too brittle to perform tensile tests. The molecular weights of H-PDMS-H also influenced the network structure and mechanical performance. The brittleness of the foam increased as the PDMS chain length was reduced; mixtures of spacer lengths ameliorated the performance (F-4B, F-11, and F-13, Table 4).[68]

Table 4. The tensile test for lignin-silicone foams

No.	Lignin content %	PHMS content %	Modulus /MPa	Tensile strength/MPa	Elongation-at-break %
F-4 B	41	8	0.30	0.30	139
F-5	41	4	0.07	0.09	143
F-6	41	16	0.85	0.51	81
F-7	41	24	-[b]	-[b]	-[b]
F-8	15	4.4	-[c]	-[c]	-[c]
F-9	25	5	0.13	0.23	249
F-11[d]	41	8	0.38	0.40	111
F-13[e]	41	8	0.42	0.54	147

[a] Tensile strength at break [b] Tensile test failed due to sample brittleness. [c] Tensile test failed due to sample torn at loading. [d] DMS-H25 was used as the spacer. [e] Silicone spacer contains 26% DMS-H25, 48% H31, and 26% H41. The modulus and elongation-at-break were obtained from averaging 3 repetitions of the tensile test.

The impact of morphology on mechanical performance (at macroscopic level): Compared with the factors discussed above, foam morphology plays a much stronger role in determining mechanical performance. The results of DMA and tensile test demonstrated that the homogenous closed cell foams Type B1 and B2 (Fig. 1) had better performance that balanced strength and elongation-at-break, which were comparable to some silicone elastomer foams (tensile strength ~ 0.20 MPa).[69] By contrast, the Type A1 foams (F-5, 8 and 11) were easy to break due to the defects of large voids (Table 4); Type A2 is better described as an elastomer than foam (that was also easy to break due to the distributed large void

defects). Type C was much more tough (Type C1) and rigid (Type C2) than type B foams.

Thermal mechanical performance of lignin-silicone foams: Silicone polymers exhibit excellent mechanical performance across a wide temperature range, from -100 to 316 °C. By contrast, the decomposition of lignin usually starts near 170 °C (TGA, ESI†). Therefore, an examination of thermal mechanical performance of lignin-silicone foams at higher temperature was necessary.

As shown in Table 3, the mechanical performance of lignin-silicone foams was improved, as shown by increased storage and loss moduli, after post-curing at 140 °C for 12 hours as a consequence of secondary crosslinking through the oxidative/hydrolytic cleavage of Si-H groups. However, the values of storage and loss moduli at T_m + 50 °C dropped if higher temperatures or longer post cures were used (post-curing temperature beyond 170 °C, Table 3). Under these conditions, further oxidation and condensation of Si-H to Si-OH and dimerization, or condensation with lignin or repolymerization of lignin, resulted in a significant increase in crosslinking density and, consequently, brittleness.[50, 59]

The fabrication of lignin-silicone foams via Piers-Rubinsztajn (PR) reaction is beneficial with respect to for its efficiency, simple formulations and processing. Compared to other lignin-based composites, especially lignin-polyurethane foams, no pretreatment on lignin (e.g., removing high molecular weight lignin fractions[38], or pre-liquefying lignin with poly(ethylene glycol[36]) was required to obtain flexible, closed cell, lignin-reinforced foams. The properties of the foam are readily tuned by formulation. The foam silicone products offer similar performance in thermal stability to polyurethane, and the materials are far more flexible, even with higher lignin content. The process itself is advantageous because no additional blowing agents are required.[35]

Softwood is readily incorporated into silicones to make elastomeric bio-composites.[19] A simple extrusion process can be used to efficiently mix ingredients, including lignin in up to 55 weight%. Compression molding at elevated temperatures for a few minutes leads to foams in which the lignin acts as a reinforcing filler and crosslinker. The structures of foam, and their accompanying properties, can be easily tailored by varying formulations and conditions. These facile processes give materials that serve as a more valuable alternative end use for lignin.

Conclusions

A simple and effective route for the preparation of foamed lignin-silicone composites via extrusion and compression molding was described. The formulation simply consists of hydrosilanes, BCF, and raw lignin particles: no pre-treatment is required. For processing, the reagents, including $B(C_6F_5)_3$, lignin, and silicone hydrides, were first extruded for a homogenous mixture at room temperature, and then molded under compression at elevated temperature. The morphology and uniformity of the foamed structure depends on many factors, including the content of lignin, BCF, or PHMS, the molecular weight of H-PDMS-H, and the molding temperature. The content of lignin, the reinforcing filler and crosslinker, could be varied in a wide range from 25 to 42% to give robust closed cell foams with excellent mechanical performance. The strength of the foam was improved by post-curing. The successful processing method for lignin-based bio-composite could open new pathways to the better utilization of lignin.

Acknowledgements

We acknowledge with gratitude the financial support of the Natural Sciences and Engineering Research Council of Canada (NSERC) and Sentinel: NSERC Research Network on Bioactive Paper. We thank Weyerhaeuser for the gift of softwood lignin, and the FIBRE network for providing a travel grant to JZ to permit collaborative work in France.

Notes and references

1. D. Carpenter, T. L. Westover, S. Czernik and W. Jablonski, *Green Chemistry*, 2014, 16, 384-406.
2. A. Gandini, *Macromolecules*, 2008, 41, 9491-9504.
3. T. Van de Ven and L. Godbout, *Cellulose - Medical, Pharmaceutical and Electronic Applications*, InTech, 2013.
4. K. Benhamou, H. Kaddami, A. Magnin, A. Dufresne and A. Ahmad, *Carbohydrate Polymers*, 2015, 122, 202-211.
5. A. Bendahou, H. Kaddami and A. Dufresne, *European Polymer Journal*, 2010, 46, 609-620.
6. R. J. A. Gosselink, E. de Jong, B. Guran and A. Abacherli, *Industrial Crops and Products*, 2004, 20, 121-129.
7. E. Adler, *Wood Sci. Technol.*, 1977, 11, 169-218.
8. C. Heitner, D. Dimmel and J. A. Schmidt, *Lignin and Lignans: Advances in Chemistry*, Taylor & Francis, 2010.
9. X. Ma, Y. Tian, W. Hao, R. Ma and Y. Li, *Appl. Catal. A: Gen.*, 2014, 481, 64-70.
10. T. Saito, R. H. Brown, M. A. Hunt, D. L. Pickel, J. M. Pickel, J. M. Messman, F. S. Baker, M. Keller and A. K. Naskar, *Green Chemistry*, 2012, 14, 3295-3303.
11. T. Voitl and P. R. v. Rohr, *Industrial & Engineering Chemistry Research*, 2010, 49, 520-525.
12. J. D. P. Araújo, C. A. Grande and A. E. Rodrigues, *Chemical Engineering Research and Design*, 2010, 88, 1024-1032.
13. I. A. Pearl, *Journal of the American Chemical Society*, 1942, 64, 1429-1431.
14. H. Chung and N. R. Washburn, *ACS Applied Materials & Interfaces*, 2012, 4, 2840-2846.
15. D. Feldman, M. Lacasse and R. St. J. Manley, *Journal of Applied Polymer Science*, 1988, 35, 247-257.
16. C. Ciobanu, M. Ungureanu, L. Ignat, D. Ungureanu and V. I. Popa, *Industrial Crops and Products*, 2004, 20, 231-241.
17. T. Saito, J. H. Perkins, D. C. Jackson, N. E. Trammel, M. A. Hunt and A. K. Naskar, *RSC Advances*, 2013, 3, 21832-21840.
18. H. Nadji, C. Bruzzèse, M. N. Belgacem, A. Benaboura and A. Gandini, *Macromolecular Materials and Engineering*, 2005, 290, 1009-1016.
19. A. Gandini, M. Belgacem, Z.-X. Guo and S. Montanari, in *Chemical Modification, Properties, and Usage of Lignin*,

ed. T. Hu, Springer US, 2002, DOI: 10.1007/978-1-4615-0643-0_4, ch. 4, pp. 57-80.
20. B. Zhao, G. Chen, Y. Liu, K. Hu and R. Wu, *Journal of Materials Science Letters*, 2001, 20, 859-862.
21. K. Hofmann and W. G. Glasser, *Journal of Wood Chemistry and Technology*, 1993, 13, 73-95.
22. J. Qin, M. Woloctt and J. Zhang, *ACS Sustainable Chemistry & Engineering*, 2013, 2, 188-193.
23. T. N. M. T. Ismail, H. A. Hassan, S. Hirose, Y. Taguchi, T. Hatakeyama and H. Hatakeyama, *Polym. Int.*, 2010, 59, 181-186.
24. A. Tejado, C. Peña, J. Labidi, J. M. Echeverria and I. Mondragon, *Bioresource Technology*, 2007, 98, 1655-1663.
25. A. Donmez Cavdar, H. Kalaycioglu and S. Hiziroglu, *Journal of Materials Processing Technology*, 2008, 202, 559-563.
26. Y.-L. Chung, J. V. Olsson, R. J. Li, C. W. Frank, R. M. Waymouth, S. L. Billington and E. S. Sattely, *ACS Sus. Chem. Eng.*, 2013, 1, 1231-1238.
27. M. Thunga, K. Chen, D. Grewell and M. R. Kessler, *Carbon*, 2014, 68, 159-166.
28. W. Thielemans, E. Can, S. S. Morye and R. P. Wool, *Journal of Applied Polymer Science*, 2002, 83, 323-331.
29. D. S. Argyropoulos, H. Sadeghifar, C. Cui and S. Sen, *ACS Sustainable Chemistry & Engineering*, 2013, 2, 264-271.
30. Z.-X. Guo, A. Gandini and F. Pla, *Polymer International*, 1992, 27, 17-22.
31. Y. Li and A. J. Ragauskas, *RSC Advances*, 2012, 2, 3347-3351.
32. X. Pan and J. Saddler, *Biotechnology for Biofuels*, 2013, 6, 12.
33. B.-L. Xue, J.-L. Wen and R.-C. Sun, *ACS Sus. Chem. Eng.*, 2014, 2, 1474-1480.
34. C. Cateto, F. Barreiro, A. Rodrigues and N. Belgacem, *AIP Conference Proceedings*, 2008, 1042, 243-245.
35. Y. Li and A. J. Ragauskas, *Journal of Wood Chemistry and Technology*, 2012, 32, 210-224.
36. P. Cinelli, I. Anguillesi and A. Lazzeri, *European Polymer Journal*, 2013, 49, 1174-1184.
37. H. Yoshida, R. Mörck, K. P. Kringstad and H. Hatakeyama, *Journal of Applied Polymer Science*, 1987, 34, 1187-1198.
38. H. Yoshida, R. Mörck, K. P. Kringstad and H. Hatakeyama, *Journal of Applied Polymer Science*, 1990, 40, 1819-1832.
39. G. Moad, *Prog. Polym. Sci.*, 2011, 36, 218-237.
40. P. N. Bhandari, D. D. Jones and M. A. Hanna, *Carbohydrate Polymers*, 2012, 87, 2246-2254.
41. J. H. Bridson, D. J. van de Pas and A. Fernyhough, *J. Appl. Polym. Sci.*, 2013, 128, 4355-4360.
42. M. E. Carr, *J. Appl. Polym. Sci.*, 1991, 42, 45-53.
43. S. Kubo and J. F. Kadla, *Biomacromolecules*, 2003, 4, 561-567.
44. S. Baumberger, C. Lapierre, B. Monties and G. D. Valle, *Polym. Degrad. Stabil.*, 1998, 59, 273-277.
45. E. M. Fernandes, I. M. Aroso, J. F. Mano, J. A. Covas and R. L. Reis, *Composites Part B: Engineering*, 2014, 67, 371-380.
46. G. Stiubianu, M. Cazacu, M. Cristea and A. Vlad, *J. Appl. Polym. Sci.*, 2009, 113, 2313-2321.
47. M. A. Brook, J. B. Grande and F. Ganachaud, *Adv. Polym. Sci.*, 2011, 235, 161–183.
48. J. Zhang, Y. Chen and M. A. Brook, *ACS Sus. Chem. Eng.*, 2014, 2, 1983-1991.
49. E. Feghali and T. Cantat, *Chemical Communications*, 2014, 50, 862-865.
50. J. Zhang, Y. Chen, P. Sewell and M. A. Brook, *Green Chemistry*, 2015, 17, 1811-1819.
51. V. Gevorgyan, M. Rubin, S. Benson, J.-X. Liu and Y. Yamamoto, *J. Org. Chem.*, 2000, 65, 6179-6186.
52. M. Brook, J. Grande and F. ß. Ganachaud, in *Silicon Polymers*, ed. A. M. Muzafarov, Springer Berlin Heidelberg, 2011, vol. 235, ch. 47, pp. 161-183.
53. J. J. Chruściel and E. Leśniak, *J. Appl. Polym. Sci.*, 2011, 119, 1696-1703.
54. K. C. Frisch, *Journal of Macromolecular Science: Part A - Chemistry*, 1981, 15, 1089-1112.
55. L. J. Lee, C. Zeng, X. Cao, X. Han, J. Shen and G. Xu, *Composites Sci. Tech.*, 2005, 65, 2344-2363.
56. Y. Zhou, S. Wang, Y. Zhang, Y. Zhang, X. Jiang and D. Yi, *J. Appl. Polym. Sci.*, 2006, 101, 3395-3401.
57. M. Brook, J. Grande and F. Ganachaud, in *Silicon Polymers*, ed. A. M. Muzafarov, Springer Berlin Heidelberg, 2011, vol. 235, ch. 47, pp. 161-183.
58. J. M. Blackwell, K. L. Foster, V. H. Beck and W. E. Piers, *J. Org. Chem.*, 1999, 64, 4887-4892.
59. J. Li, G. Henriksson and G. Gellerstedt, *Bioresource Technology*, 2007, 98, 3061-3068.
60. S. K. Thanawala and M. K. Chaudhury, *Langmuir*, 1999, 16, 1256-1260.
61. A. Chien, R. S. Maxwell, S. DeTeresa, L. Thompson, R. Cohenour and B. Balazs, *J. Polym. Sci. B, Polym. Phys.*, 2006, 44, 1898-1906.
62. N. Bosq, N. Guigo, J. Persello and N. Sbirrazzuoli, *Phys. Chem. Chem. Phys.*, 2014, 16, 7830-7840.
63. R. Kosfeld and M. Heß, in *Anwendungsbezogene physikalische Charakterisierung von Polymeren, insbesondere im festen Zustand*, eds. E. W. Fischer, F. H. Müller and R. Bonart, Steinkopff, 1979, vol. 66, ch. 6, pp. 43-50.
64. M. H. Lacoste-Ferré, P. Demont, J. Dandurand, E. Dantras, M. Blandin and C. Lacabanne, *J. Mater. Sci.*, 2006, 41, 7611-7616.
65. V. Darras, O. Fichet, F. Perrot, S. Boileau and D. Teyssié, *Polymer*, 2007, 48, 687-695.
66. W. Liu, R. Zhou, H. L. S. Goh, S. Huang and X. Lu, *ACS Applied Materials & Interfaces*, 2014, 6, 5810-5817.
67. M. J. Schroeder and C. M. Roland, *Macromolecules*, 2002, 35, 2676-2681.
68. K. H. Schimmel and G. Heinrich, *Colloid Polym Sci*, 1991, 269, 1003-1012.
69. D. Blanc and D. Canpont, Google Patents, 2011.

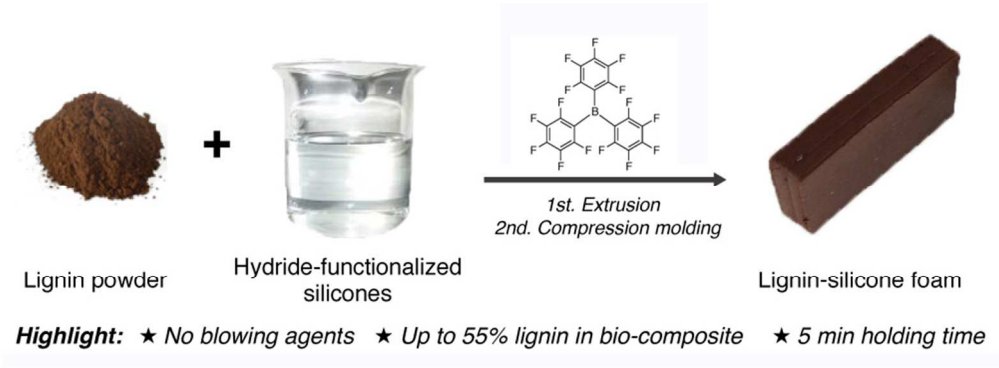

Graphical Abstract: Lignin-reinforced foams are efficiently prepared in a compression mold.
85x31mm (300 x 300 DPI)